

# Synthesis, one and two-photon optical properties of two asymmetrical and symmetrical carbazole derivatives containing quinoline ring



Liang Li<sup>a</sup>, Ping Wang<sup>b</sup>, Yichi Zhang<sup>b</sup>, Yiqun Wu<sup>a,b,\*</sup>, Zhimin Chen<sup>b</sup>, Chunying He<sup>b</sup>

<sup>a</sup> Shanghai Institutes of Optics and Fine Mechanics, Chinese Academy of Sciences, No. 390, Qinghe Road, Jiading District, Shanghai 201800, China  
<sup>b</sup> Key Lab of Functional Inorganic Material Chemistry, Heilongjiang University, Ministry of Education, Harbin 150080, China

## HIGHLIGHTS

- Novel carbazole derivatives containing quinoline were synthesized.
- Electronic transition of carbazole derivatives were theoretically studied by TD-DFT.
- Long fluorescence lifetime of carbazole derivatives was obtained.
- Two-photon absorption of compounds was measured by 120 fs pulse at 800 nm.

## ARTICLE INFO

### Article history:

Received 7 March 2013  
 Received in revised form 19 July 2013  
 Accepted 24 July 2013  
 Available online 31 July 2013

### Keywords:

Carbazole derivatives  
 One and two-photon optical properties  
 Quinoline ring

## ABSTRACT

The carbazole derivatives are suitable for two-photon absorption optical storage and photoluminescence material. Two carbazole derivatives, asymmetrical and symmetrical type molecules containing quinoline rings as electron acceptors and an N-ethylcarbazole group as electron donor, 9-ethyl-3-(2-quinolin)vinyl-carbazole (**4**) and 9-ethyl-3,6-bis(2-(quinolin)vinyl)-carbazole (**5**), had been synthesized by the Vilsmeier reaction of formylation and Knoevenagel condensation. The one-photon properties including absorption, fluorescence emission spectra, fluorescence quantum yields and fluorescence decay behaviors were investigated in N,N-dimethylformamide. Meanwhile, these compounds were theoretically surveyed by the density functional theory (DFT) and the time-dependent functional theory (TD-DFT). The two-photon excited fluorescence and two-photon absorption cross-sections were measured for the compounds by 120 fs pulse at 800 nm Ti: sapphire laser operating at 1 kHz repetition rate. The results showed that both of the two compounds **4** and **5** had higher fluorescence quantum yield ( $\Phi$ ) of 0.77 and 0.81 comparing with carbazole. Compound **5** with symmetric  $\pi$  conjugated structure possessed longer fluorescence lifetime ( $\tau$ ) of 21.4 ns and larger two-photon absorption cross-sections ( $\delta_{\text{TPA}}$ ) of  $364 \times 10^{-50} \text{ cm}^4 \text{ s/photon}$  than those of compound **4** with asymmetric  $\pi$  conjugated structure ( $\tau = 10.03 \text{ ns}$  and  $\delta_{\text{TPA}} = 81 \times 10^{-50} \text{ cm}^4 \text{ s/photon}$ ). It was indicated that the one and two-photon optical properties of carbazole derivatives are influenced strongly by the symmetry and length of  $\pi$  conjugated structure.

© 2013 Elsevier B.V. All rights reserved.

## 1. Introduction

Two-photon absorption (TPA) is a phenomenon that involves the excitation of a molecule by simultaneous absorption of two-photons [1]. Therefore, two-photon absorption (TPA) holds a great potential for a number of industrial and medical applications such as optical power limiting [2–5], two-photon up-conversion lasing [6,7], two-photon fluorescence excitation microscopy [8–12], three-dimensional (3D) optical data storage and microfabrication [13–18]. For all the applications mentioned above, it is highly

desirable to employ molecules with a large TPA cross section. For this requirement, research in both experimental and theoretical ways for obtaining the structure–property relation has been pushed forward [19–22]. In exploring strong TPA compounds, Albota et al. had focused on symmetric intramolecular charge transfer organic molecules and emphasized the importance of conjugation length, donor/acceptor strength, and molecular symmetry [23]. Meanwhile, Reinhardt et al. had also respectively studied the effects of the planarity of  $\pi$ -center, donor strength, and molecular asymmetry on asymmetric intramolecular charge transfer ones [24]. The available research results exhibited that the conjugation length, donor–acceptor functionalities, conformation, orientation of the molecule, the molecular dimensionality, molecular congregating effects, etc. are significant factors to be considered in the molecular design and synthesis [20,21].

\* Corresponding author at: Shanghai Institutes of Optics and Fine Mechanics, Chinese Academy of Sciences, No. 390, Qinghe Road, Jiading District, Shanghai 201800, China. Tel.: +86 21 69918592/8087; fax: +86 21 69918562.

E-mail address: [yqwu@siom.ac.cn](mailto:yqwu@siom.ac.cn) (Y. Wu).

It is well known that carbazole is isoelectronic to diphenylamine, but it has a planar structure and it can be imagined as the bonded diphenylamine. The carbazole nucleus can be easily functionalized at 3-, 6-, 9-positions and covalently linked to other molecular groups [25]. Typical push–pull chromophores consist of a polar A– $\pi$ –D system with a planar  $\pi$ -system end-capped by a strong electron donor (D) and a strong electron acceptor (A). In order to ensure intramolecular charge transfer (ICT) between the donor (D = N-alkyl group etc.) and the acceptor (A = cyano group etc.), double or triple bonds is the most common methods of linking the  $\pi$ -conjugated system between aromatic and hetero-aromatic rings [26,27]. Carbazole moiety being a rigid structure with a donor-rigidised residue improves  $\pi$ -electron delocalization resulting in better two-photon absorbing property [28]. Up to now, many research groups have reported the structures, optical and electronic properties of many carbazole derivatives because of their excellent advantages of chemical, thermal and photochemical stabilities as well as their ease adjustment of the electronic and optical properties [29–35]. It is very important for the applications of carbazole derivatives as optical materials to understand the relations between the optical properties and molecule structure, especially the effect of  $\pi$ -conjugated structure on the optical properties of carbazole derivatives. In this paper, two carbazole derivatives, asymmetrical and symmetrical type molecule containing quinoline rings as electron acceptors and an N-ethylcarbazole group as electron donor, 9-ethyl-3-(2-quinolin)viny-carbazole and 9-ethyl-3,6-bis(2-(quinolin)viny)-carbazole, have been synthesized by the Vilsmeier reaction of formylation and Knoevenagel condensation. Linear absorption spectra, one-photon excited fluorescence, fluorescence quantum yields and fluorescence decay behaviors of the compounds are investigated. Density functional theory (DFT) and time-dependent functional theory (TD-DFT) are utilized to survey theoretically the electron transition feature. The two-photon excited fluorescence of the compounds are studied by 120 fs pulse at 800 nm Ti: sapphire laser operating at 1 kHz repetition rate and two-photon absorption cross-section is measured. The effect of  $\pi$ -conjugated structure containing quinoline rings as electron acceptors and an N-ethylcarbazole group as electron donors on the one and two-photon optical properties of the carbazole derivatives is discussed as well.

## 2. Experimental

### 2.1. Instrumentation

<sup>1</sup>H NMR spectra were recorded in CDCl<sub>3</sub> on a Bruker AVANCE-300 MHz NMR instrument using TMS as internal standard. IR spectra were recorded using Perkin Elmer FT-IR System. The spectra of the solid compounds were performed in the form of KBr pellets. Mass spectra were obtained with a Bruker Agilent 6890-5973 MALDI-TOF mass spectrometer. Elemental analyses were performed using a PE2400 elemental analyzer. Melting points were determined on  $\alpha$ -5 melting point detector.

### 2.2. Synthesis

#### 2.2.1. Synthesis of materials

The synthetic route is outlined in Scheme 1. Carbazole was halogenated by bromobutane in alkaline condition. Compound 2 and 3 were synthesized by the Vilsmeier reaction of formylation from 9-alkyl-carbazole. 9-ethyl-3-(2-(quinolin-2-yl) vinyl)-carbazole (**4**) and 9-butyl-3,6-bis(2-(quinolin)viny)-carbazole (**5**) were synthesized using Knoevenagel condensation. 9-ethyl-carbazole (**1**), 9-ethyl-3-formyl-carbazole (**2**) and 3,6-diformyl-9-ethyl-carbazole (**3**) were synthesized by the reported procedure [36]. The

synthesized target compounds were identified by the measurements of <sup>1</sup>H NMR, IR and MS, and are in agreement with the chemical structures shown in Scheme 1.

#### 2.2.2. Synthesis of 9-ethyl-3-(2-quinolin)viny-carbazole (**4**)

3-Formyl-9-ethyl-carbazole (1.784 g, 8 mmol) and 2-methyl-quinoline (1.144 g, 8 mmol) were added in 50 ml acetic anhydride. The reaction mixture was heated to 120 °C and refluxed for 36 h. After the reaction, when cooled it to room temperature, the reaction solution was poured into water, and adjusted its pH to neutral with alkaline solution. Then it was extracted with dichloromethane for three times to yield a crude sample. The product **4** was purified through column chromatography on silica gel using ethyl acetate–petroleum ether (1:4) as eluent.

**9-ethyl-3-(2-quinolin)viny-carbazole (**4**)**, yield: 48.3%, M.P. 286 °C;  $\lambda_{\max}$  = 294 nm; <sup>1</sup>H NMR(CDCl<sub>3</sub>):  $\delta$ (ppm) 1.3(t, 3H, CH<sub>3</sub>), 4.5(m, 2H, CH<sub>2</sub>), 7.2(m, 2H, CH=CH), 7.4–8.4(m, 13H, carbazole); IR(KBr): 2950, 2925, 1610, 1496, 1465, 1424, 1381, 1327, 1213, 966, 820 cm<sup>-1</sup>; Anal. calcd(%) for C<sub>25</sub>H<sub>20</sub>N<sub>2</sub>: C, 86.21; H, 5.75; N, 8.04. Found: C, 85.67; H, 6.14; N, 8.19; LC-MS: *m/z*, 349.1(348.16) [M + 1].

#### 2.2.3. Synthesis of 9-ethyl-3,6-bis(2-(quinolin)viny)-carbazole (**5**)

3,6-dicarbaldehyde-9-ethyl-carbazole (2.008 g, 8 mmol) and 2-methyl-quinoline (6.864 g, 48 mmol) were added in 100 ml acetic anhydride. The reaction mixture was heated to 120 °C and refluxed for 36 h. After the reaction, when cooled it to room temperature, the reaction solution was poured into water, and adjusted its pH to neutral with alkaline solution. Then it was extracted with dichloromethane for three times to yield a crude sample. The product **5** was purified through column chromatography on silica gel using ethyl acetate–petroleum ether (1:6) as eluent.

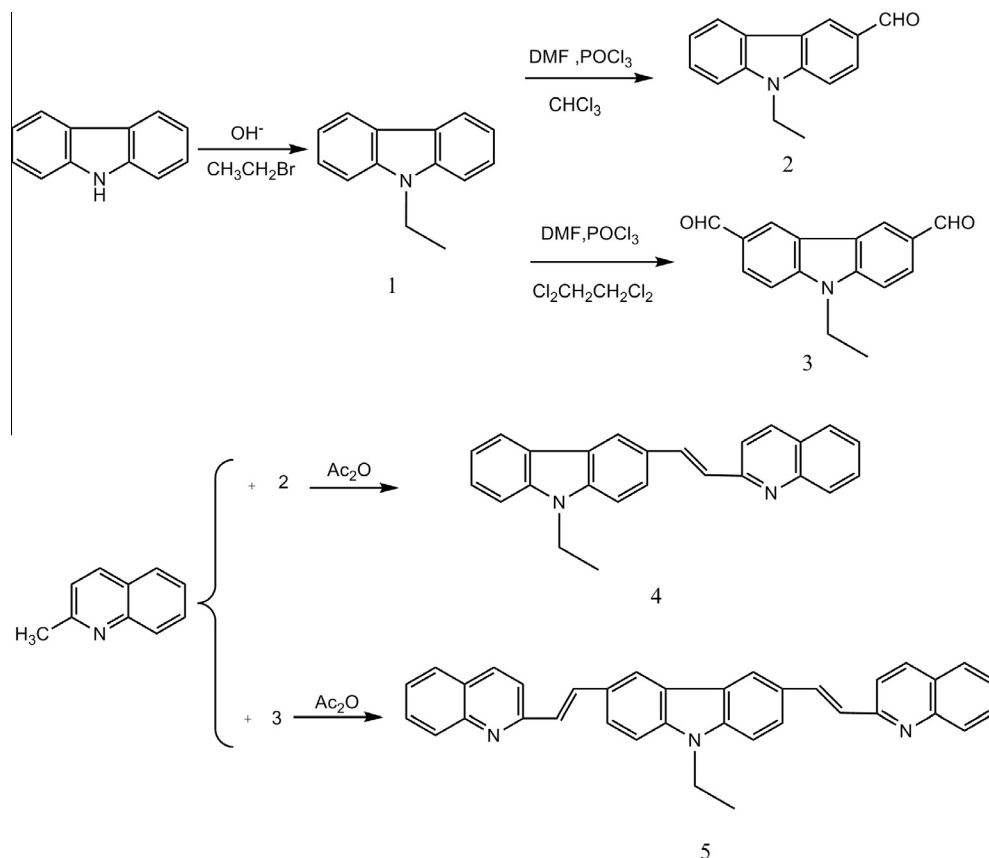
**9-ethyl-3,6-bis(2-(quinolin)viny)-carbazole (**5**)**, yield 43.1%. M.P. 271 °C;  $\lambda_{\max}$  = 296 nm; <sup>1</sup>H NMR(CDCl<sub>3</sub>):  $\delta$ (ppm) 1.5 (t, 3H, CH<sub>3</sub>), 4.4(m, 2H, CH<sub>2</sub>), 7.2 (m, 4H, CH=CH), 7.4–8.4(m, 18H, carbazole); IR(KBr): 3037, 2955, 2929, 1589, 1501, 1483, 1426, 1381, 1312, 1232, 964, 819 cm<sup>-1</sup>; Anal. calcd(%) for C<sub>36</sub>H<sub>27</sub>N<sub>3</sub>: C, 86.23; H, 5.39; N, 8.38. Found: C, 85.46; H, 6.12; N, 8.42; LC-MS: *m/z*, 502.2(501.22) [M + 1].

### 2.3. One-photon optical properties measurements

The linear absorption spectra were measured in DMF at a concentration of  $c = 1.0 \times 10^{-5}$  mol/dm<sup>3</sup>, in which the solvent influence was not included. The linear absorption spectra of the compounds were obtained by a Perkin Elmer Lambda 900UV/Vis/NIR (San Jose, California, USA) spectrophotometer. One-photon fluorescence spectra were measured at room temperature. Fluorescence decay curves were recorded with the lifetime combined single-photon counting technique using a commercially available Edinburgh Instruments, model LS-55 spectrometer equipped with a 375 nm picosecond pulse diode laser made in Britain. The fluorescence quantum yield  $\Phi_{\chi} = (A_s \times F_{\chi} \times n_s^2 \times \Phi_s) / (A_{\chi} \times F_s \times n_{\chi}^2)$  where  $A$  denotes the absorbance at the excitation wavelength,  $F$  means the area under the fluorescence curve and  $n$  is the refraction index. Subscripts  $s$  and  $\chi$  refer to the standard and to the sample of unknown quantum yield, respectively. Rhodamine B in ethanol at 25 °C ( $\Phi = 0.9$ ) was made as the standard.

### 2.4. Two-photon fluorescence measurements

In order to explore the TPA properties of the target compounds, we use two-photon excited fluorescence method to measure the TPA cross section by laser [37,38]. The experimental setup is shown in Fig. 1. The two-photon fluorescence spectra of the compounds are investigated by a 120-fs 800-nm pulse Ti: sapphire



**Scheme 1.** The synthetic route of the target compounds.

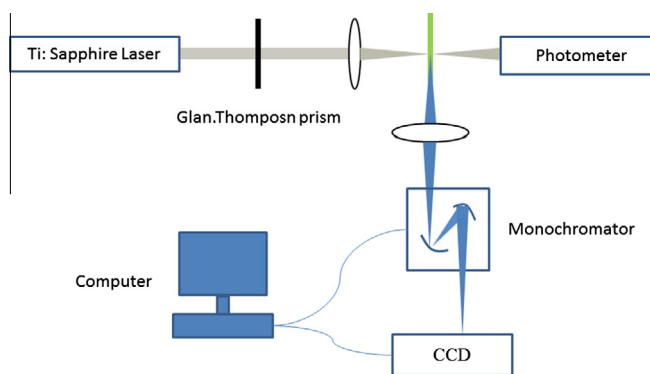


**Fig. 1.** Experimental setup for two-photon excited fluorescence.

femto-second laser operating at 1 kHz repetition rate in the DMF at a concentration of  $1.0 \times 10^{-3}$  mol/dm<sup>3</sup>. The fluorescence spectra are recorded by a 16-bit CCD (Jobin-Yvon, Horiba, France) that mounted at the output of the monochromator.

### 2.5. Computational procedures

All calculations are performed using Gaussian 03 W. The geometry optimizations of the electronic ground state are carried out at the density functional theory (DFT) level [37,38] with the hybrid Becke, three-parameter, Lee–Yang–Parr (B3LYP) exchange correlation functional [39,40], and the split-valence 6-31G\* basis set [41]. DFT/B3LYP/6-31G\* has been reported to be an accurate formalism for calculating the structural properties of many molecular systems [36,42]. Time-dependent functional theory (TD-DFT) is used

to research singlet–singlet electronic transition for these molecules.

## 3. Results and discussion

### 3.1. One-photon absorption and fluorescence emission spectra

The one-photon absorption and emission spectra of carbazole, 4 and 5 in DMF are shown in Fig. 2. The  $\pi \rightarrow \pi^*$  character absorption peaks of the carbazole derivatives 4 and 5 locate at 360 nm and

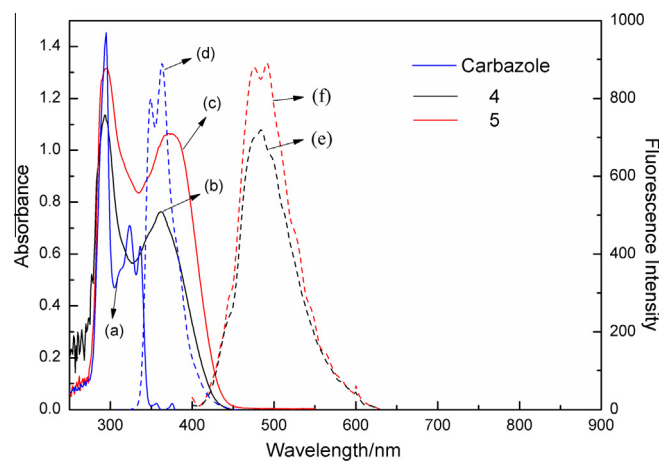


**Fig. 2.** (a–c) are linear absorption of carbazole, 4 and 5 in DMF ( $d_0 = 1.0 \times 10^{-5}$  mol dm<sup>-3</sup>); (d–f) are fluorescence intensity of carbazole, 4 and 5 in DMF ( $d_0 = 1.0 \times 10^{-5}$  mol dm<sup>-3</sup>).

372 nm, respectively. The  $\lambda_{\text{absmax}}$  of the two compounds present an  $n \rightarrow \pi^*$  character at 294 nm and 296 nm and display a slight red-shift compared with the maximum absorption peaks of carbazole (at 282 nm). Meanwhile, compared to the asymmetric structure of compounds 4, the conjugation length of compounds 5 is increased by modified quinoline ring on the 3, 6- of the bilateral carbazole unit and the 372 nm absorption peaks ( $\lambda_{\text{abs}}$ ) of compounds 5 happen red-shifted 12 nm because of its disubstituted at 3, 6-position to form a symmetry A- $\pi$ -D- $\pi$ -A type structure. Furthermore, the absorption spectra of the compounds show that there is no linear absorption in the range of 450–900 nm, which would be a wide window for investigating the two-photon optical properties.

In Fig. 2, c and d show the fluorescence emission spectra of samples 4 and 5 in the DMF at a concentration of  $1.0 \times 10^{-5}$  mol dm<sup>-3</sup> respectively. The  $\lambda_{\text{excmax}}$  and  $\lambda_{\text{flu}}$ , as well as the fluorescence quantum yields of 4 and 5 in DMF are shown in Table 1. The  $\lambda_{\text{flu}}$  fluorescence wavelengths of 4 and 5 are at 484 and 492 nm, locating the blue–green spectral range. They are greatly red-shifted more than 124 nm compared with the  $\lambda_{\text{flu}}$  fluorescence wavelengths of carbazole (at 368 nm). It is found that absorption and fluorescence spectra have nearly mirror-image profiles. From Table 1, the  $\Delta\lambda_{\text{Stokes}}$  of 4 and 5 correspond to 91, and 94, respectively. The fluorescence quantum yields  $\Phi$  of the compounds 4 and 5 are 0.77 and 0.81 in the DMF, which are equivalent to 6.4 and 6.8 times that of carbazole (0.12). Fluorescence quantum yields  $\Phi$  can be greatly enhanced by introducing quinoline ring on the position of 3 or 3, 6 of the carbazole unit to increase the  $\pi$ -conjugation length. The fluorescence decay behaviors of compound 4 and 5 in DMF are recorded. The fluorescence decay curves of compounds are shown in Fig. 3. The fluorescence lifetime ( $\tau$ ) is given in Table 1. It is found that both of these two carbazole derivatives 4 and 5 have long fluorescence lifetime ( $\tau$ ) of 10.03 ns and 21.4 ns, which are much longer than that of carbazole (6.66 ns). Because of the longer  $\pi$ -conjugation length, fluorescence lifetime ( $\tau$ ) of compound 5 with symmetrical structure is as twice long as that of compound 4 with asymmetrical.

### 3.2. Frontier molecular orbitals

The optimized geometry of the ground is obtained and shown in Fig. 4. It is showed that the optimized structure possesses a good planarity conjugated system, in which one- or two-quinolone ring are linked from 3 or 3, 6 of cabazole unit. The planarity is its important structure property, which is directly related to the conjugation of  $\pi$  bond system. The nature and energies of the HOMO and LUMO of the compounds, which play an important role in the photo luminescence properties of the compounds, are investigated at the DFT/B3LY/6-31G\* level. The isodensity surface plots of HOMO and LUMO are shown in Fig. 5. The HOMOs of the compounds are delocalized among the whole molecules and the distributions of the LUMO appear to be different for the two molecules. Table 2 lists the calculated HOMO and LUMO energies. The increase in the conjugated length makes the HOMO energies higher, the LUMO energies lower, and the energy gaps narrower [36]. From Table 2, it can be known that the increase of the conjugation length also results in the decrease of energy gaps ( $\Delta E$ ): 4.798 eV

**Table 1**  
Absorption, excitation and fluorescence spectra data of carbazole, 4 and 5 in DMF.

| Sample    | $\lambda_{\text{abs}}$ (nm) | $\lambda_{\text{excmax}}$ (nm) | $\lambda_{\text{flu}}$ (nm) | $\Delta\lambda_{\text{Stokes}}$ (nm) | $\Phi$            | $\tau$ (ns) |
|-----------|-----------------------------|--------------------------------|-----------------------------|--------------------------------------|-------------------|-------------|
| Carbazole | 282, 332 <sup>a</sup>       | 294 <sup>a</sup>               | 368 <sup>a</sup>            | 74 <sup>a</sup>                      | 0.12 <sup>a</sup> | 6.66        |
| 4         | 294, 360                    | 393                            | 484                         | 91                                   | 0.77              | 10.03       |
| 5         | 296, 372                    | 398                            | 492                         | 94                                   | 0.81              | 21.40       |

<sup>a</sup> The data are from Ref. [36].

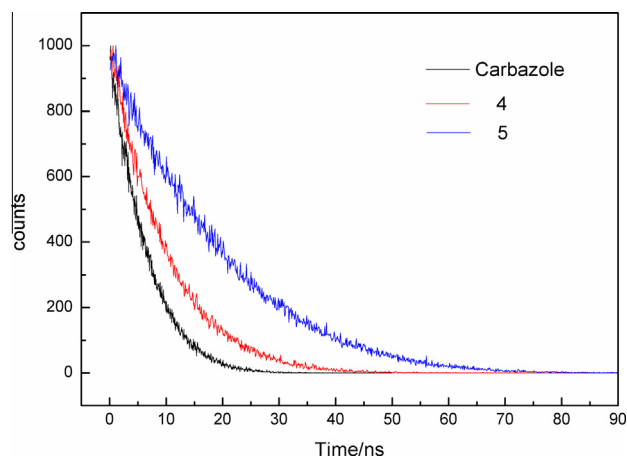


**Fig. 3.** The fluorescence decay curve of carbazole, compounds 4 and 5 in DMF.

(Carbazole) > 3.461 eV (Compound 4) > 3.287 eV (Compound 5), which indicate that introducing quinoline ring on the 3,6-of the bilateral carbazole unit is more favorable for the stability of molecular systems.

To aid the interpretation of our experimental results, we have carried out a theoretical study to determine the equilibrium geometry of the molecules, as well as to predict their electronic transitions, either related to one-photon absorption. All the theoretical computations for singlet–singlet electronic transition are carried out within the DFT framework. TD-DFT has been assumed at vacuum conditions to calculate the absorption spectrum. The theoretical results for one-photon absorption (OPA) of compound 4 and 5 are displayed in Table 3, which include transitions energies ( $E$ ), oscillator strengths ( $f$ ) and main configurations. From Table 3, it is observed that the first electronic transition via theoretical calculation for compound 4 occurs at 365 nm, which is almost consistent experimental result ( $\lambda_{\text{ab}} = 360$  nm), seen in Fig. 2. Analysis of the molecular orbitals of compound 4 indicates that the main excitation from the highest occupied molecular orbital (HOMO) to the lowest unoccupied molecular orbital (LUMO) has a  $\pi \rightarrow \pi^*$  character. On the other hand, the theoretical electronic transition ( $\lambda_{\text{ab}} = 370$  nm,  $f = 0.575$ ) for compound 5 allow  $\pi \rightarrow \pi^*$  transition, corresponding now to HOMO<sub>-1</sub>  $\rightarrow$  LUMO<sub>+1</sub> transition, which is almost in good agreement with the 372 nm obtained in the experimental results (in Fig. 2). The remaining calculated transitions present low oscillator strength and cannot be observed in the linear absorption spectrum.

### 3.3. Two-photon absorption properties

Based on the two-photon (TPA) excited fluorescence method of studying TPA property, the intensity  $I_f$  of fluorescence induced by two-photon excitation determined by laser intensity  $I_0$  and the total number of molecules  $N$  is given by the following equation [37]:

$$I_f = C I_0^2 N \quad (1)$$

where  $C$  is a constant. Pulsed intensities at the geometric focal point are calculated using the following equation:

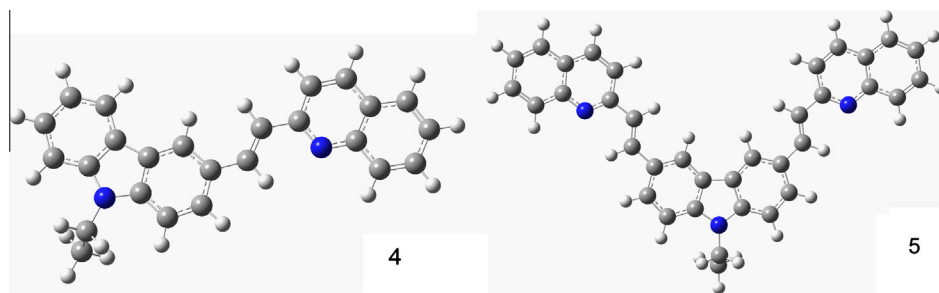


Fig. 4. The optimized geometry of the ground state of the compound 4 and 5.

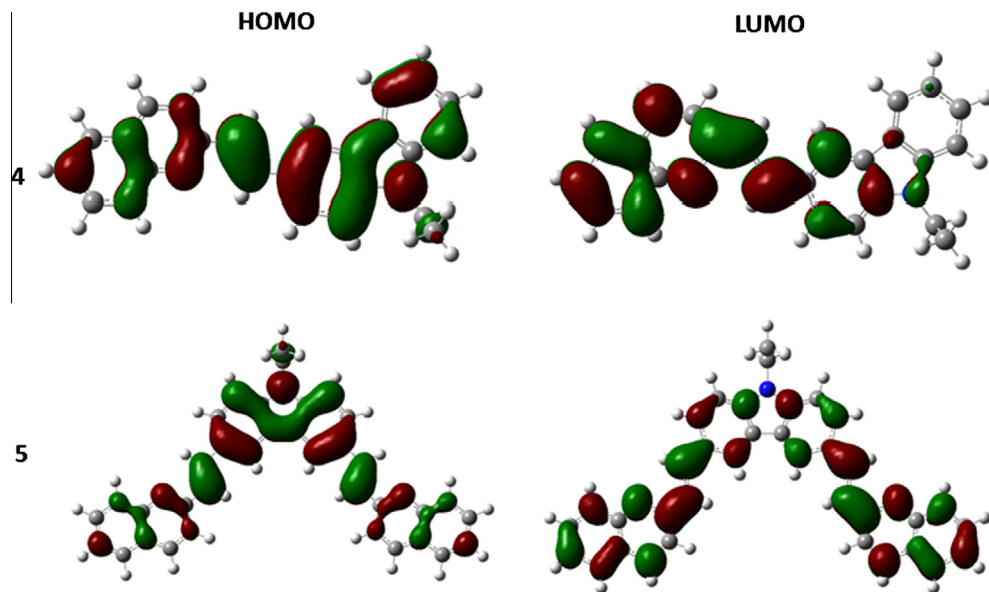


Fig. 5. Plots of HOMO and LUMO of 4 and 5 by DFT//B3LYP/6-31G\*.

**Table 2**  
Negative of the HOMO ( $-\epsilon_{\text{HOMO}}$ ) and LUMO ( $-\epsilon_{\text{LUMO}}$ ) energies, calculated by TD-DFT.

| Molecule              | $-\epsilon_{\text{HOMO}}$ (eV) | $-\epsilon_{\text{LUMO}}$ (eV) | $\Delta E$ |
|-----------------------|--------------------------------|--------------------------------|------------|
| Cabazole <sup>a</sup> | 5.4427                         | 0.6444                         | 4.798      |
| 4                     | 5.0558                         | 1.5948                         | 3.461      |
| 5                     | 5.0177                         | 1.7300                         | 3.287      |

<sup>a</sup> The data from Ref [36].

$$I_0(t) = \frac{\pi(N.A.)^2}{\lambda^2} P(t) \quad (2)$$

where  $N.A. = n \sin \theta$ ,  $\theta$  is the half-angle of collection for the lens,  $I_0$  means the intensity at the geometric focal point, and  $P$  refers to the incident power. So, using the formula  $I_f = C I_0^2 N$  for dealing with logarithms, the linear relation between the logarithm of the fluorescence intensity and of input power can be attained; the slope of the line should be 2 to confirm whether the process has a TPA mechanism.

The two-photon fluorescence spectra of samples 4 and 5 in the DMF are shown in Fig. 6a and b. They pumped by a femtosecond

laser pulse at 800 nm using different input power. To make sure that the collected light signal is not from other absorption mechanisms, but from the fluorescence after TPA, we adjust the input power and record the intensity dependence of the fluorescence. Meanwhile, the logarithm of the fluorescence intensity as the vertical axis is plotted with the logarithm of input power as the abscissa, shown in the insert. The slopes of the line are 1.94 and 1.96, respectively, which confirm that TPA is the main excitation mechanism of the intense fluorescence emission at the femtosecond regime.

From Fig. 6 to know, the shape of the two-photon fluorescence emission spectra is identical with the shape of one-photon fluorescence emission spectra. And the two-photon fluorescence emission wavelengths of 4 and 5 possess a maximum at 480 nm and 482 nm. This result demonstrates that the two-photon and the one-photon fluorescence processes take place from the same final excited state. Moreover, the two-photon-induced fluorescence method is adopted to explore TPA cross sections. To study the TPA cross-section  $\delta_{\text{TPA}}$  of the two carbazole derivatives, we employ fluorescein (dissolved in water, pH = 11) as the standard ( $\Phi_{\text{Flu}} = 0.92$ ) and the value of its TPA cross-section obtain from

**Table 3**  
Electronic transition data obtained by TD-DFT ( $\lambda_{\text{ab}}$ ) for 4 and 5 at the B3LYP/6-31 G\* optimized geometry.

| Molecule | Electronic transitions | Transitions energy (eV) | $\lambda_{\text{ab}}$ (nm) | Exp. <sup>a</sup> $\lambda_{\text{ab}}$ (nm) | $f$   | Main configurations                                 |        |
|----------|------------------------|-------------------------|----------------------------|--|-------|---|--------|
| 4        | $S_0 \rightarrow S_1$  | 3.45                    | 365                        | 360  | 0.748 | HOMO $\rightarrow$ LUMO                             | 0.6320 |
| 5        | $S_0 \rightarrow S_3$  | 2.17                    | 370                        | 372  | 0.575 | HOMO <sub>-1</sub> $\rightarrow$ LUMO <sub>+1</sub> | 0.5614 |

<sup>a</sup> Exp. is experimental result.

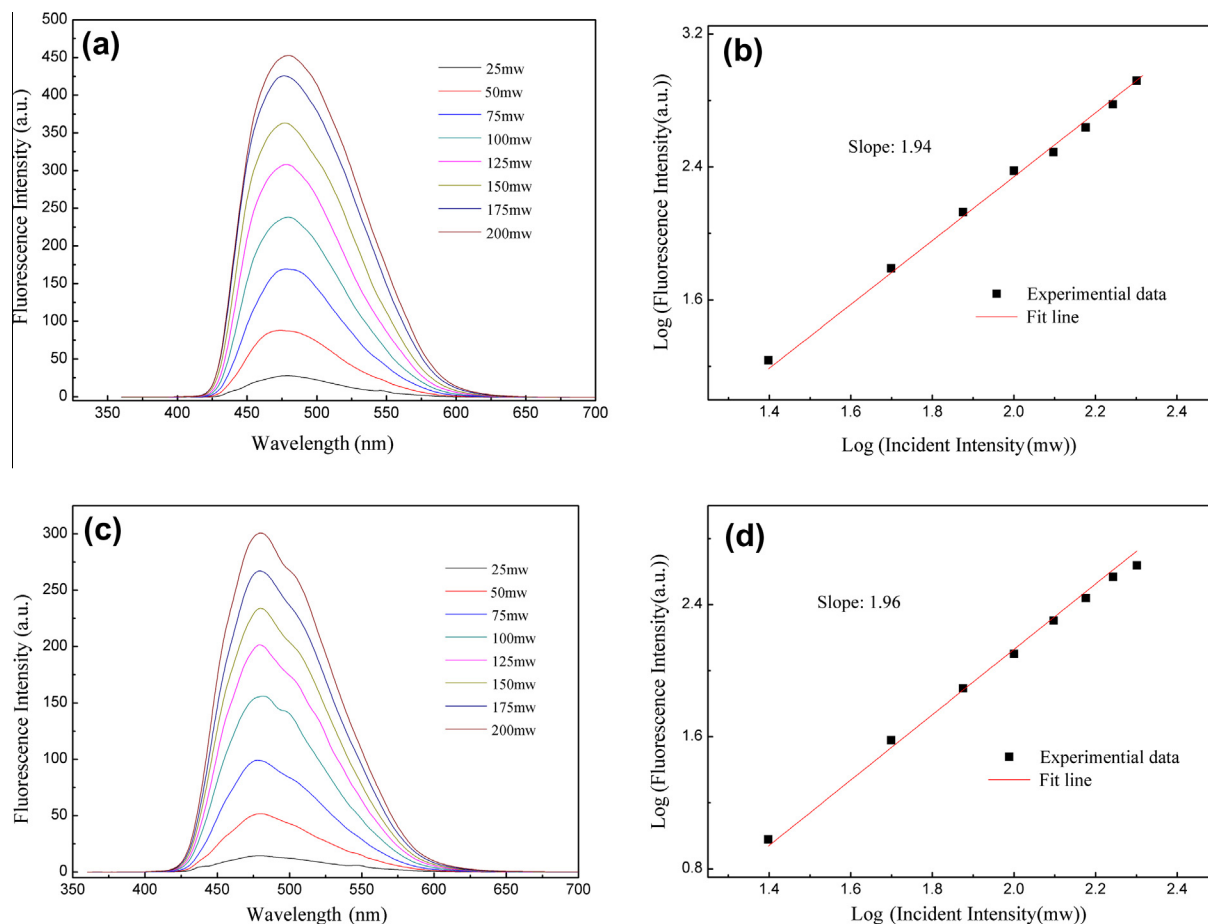


**Fig. 6.** Two-photon fluorescence for samples 4 (a) and 5 (b) in DMF pumped by femtosecond laser pulse at 800 nm using different input power; The linear graphs are the logarithm of integrate fluorescence signal of 4 (c) and 5 (d) versus logarithm of the input intensity. The black squared dots are the measured fluorescence data and the solid line is a linear fit.

Ref. [38],  $\delta_{\text{flu}} = (38.0 \pm 9.7) \times 10^{-50} \text{ cm}^4 \text{ s/photon}$ . Because the difference of the refractive index of water (1.333) and the DMF (1.4296) is small, it is neglected in the calculation. The TPA cross-section for the sample is defined as follows:

$$\delta_{\text{sample}} = \frac{\Phi_{\text{flu}}}{\Phi_{\text{sample}}} \frac{F_{\text{sample}}}{F_{\text{flu}}} \delta_{\text{flu}} \quad (3)$$

The fluorescence quantum yield of sample has been provided from its single-photon fluorescence spectrum, shown in Table 1. The following are derived:  $\delta_4 = 81 \times 10^{-50} \text{ cm}^4 \text{ s/photon}$ ;  $\delta_5 = 364 \times 10^{-50} \text{ cm}^4 \text{ s/photon}$ , which reveal that the TPA cross-section of compound 5 is more than 4 times that of compound 4. The results demonstrate that the TPA cross-sections  $\delta$  of carbazole derivatives are improved by bilateral substitution of quinoline on the 3- and 6-position of carbazole derivatives. Meanwhile, compared with  $\delta_{\text{TPA}}$  of other 9-ethyl-carbazole derivatives, the  $\delta_{\text{TPA}}$  of 9-ethyl-3,6-bis(2-(quinolin)vinyl)-carbazole (compound 5) is much larger than that of 9-ethyl-3,6-bis(styryl)-carbazole ( $\delta_{\text{TPA}} = 115 \times 10^{-50} \text{ cm}^4 \text{ s/photon}$ ) [36], which implies that if the strong acceptor quinolone group is substituted on the carbazole unit and the conjugation length is extended via the addition of a double bond between the quinolone acceptor and carbazole bridge, the TPA cross section is increased greatly.

#### 4. Conclusion

In this paper, experimental and theoretical investigation on the asymmetric-type and symmetric-type carbazole were performed

because of its great potential for application in TPA materials. Two carbazole compounds were synthesized by the Vilsmeier reaction of formylation and Knoevenagel condensation. The one and two-photon absorption properties were reported in this paper. The OPA properties of carbazole derivatives with quinoline were measured including UV-Vis spectra, fluorescence spectra and fluorescence decay behaviors. The fluorescence quantum yields (0.77 and 0.81) and fluorescence lifetime (10.03 ns and 21.4 ns) of compound 4 and compound 5 were bigger than those of carbazole, (0.12 and 6.66 ns). The TPA properties of carbazole derivatives were studied using the TPA fluorescence method with 800 nm femtosecond pulses laser. Meanwhile, the compound 5 exhibited large two-photon cross-sections,  $364 \times 10^{-50} \text{ cm}^4 \text{ s/photon}$ , with 800 nm laser excitation. Owing to the increase of the  $\pi$ -conjugation length by connecting quinoline rings from 3- and 6- of carbazole, the fluorescence decay behaviors and TPA cross-section values of the carbazole derivatives were enhanced. Based on the OPA and TPA properties, the compound may be a promising candidate material for the application in TPA three-dimension optical data storage, organic electro-luminescent and two-photon nano/micro-structure fabrication. The investigation on optical data storage of application is progressing in our laboratory, and the results will be released in the future.

#### Acknowledgements

This work was partially financially supported by the National Natural Science Foundation of China (61137002) and the Research

Fund of Heilongjiang Provincial Education Department (12511377).

## References

- [1] J. Li, X.N. Song, Y.P. Sun, C.K. Wang, *J. Mol. Struct.: THEOCHEM* 867 (2008) 53.
- [2] Y.X. Yan, X.T. Tao, Y.H. Sun, G.B. Xu, *Opt. Mater.* 27 (2005) 1787.
- [3] P.A. Fleitz, M.C. Brant, R.L. Sutherland, F.P. Strohkendl, *SPIE Proc.* 91 (1998) 3472.
- [4] G.S. He, J.D. Bhawalkar, C.F. Zhao, P.N. Prasad, *Appl. Phys. Lett.* 67 (1995) 2433.
- [5] J.E. Ehrlich, X.L. Wu, L.Y. Lee, Z.Y. Hu, *Opt. Lett.* 22 (1997) 1843.
- [6] J.D. Bhawalkar, G.S. He, P.N. Prasad, *Rep. Prog. Phys.* 59 (1996) 1041.
- [7] C.F. Zhao, G.S. He, J.D. Bhawalkar, C.K. Park, *Chem. Mater.* 7 (1995) 1979.
- [8] W. Denk, K. Svoboda, *Neuron* 18 (1997) 351.
- [9] W. Denk, *Proc. Natl. Acad. Sci. USA* 91 (1994) 6629.
- [10] C. Xu, W.R. Zipfel, J.B. Shear, R.M. William, *Proc. Natl. Acad. Sci. USA* 93 (1996) 10763.
- [11] W. Denk, J.H. Strickler, W.W. Webb, *Science* 248 (1990) 73.
- [12] R.H. Kohler, J. Cao, W.R. Zipfel, W.W. Webb, M.R. Hansen, *Science* 276 (1997) 2039.
- [13] B.H. Cumpston, S.P. Ananthavel, S. Barlow, D.L. Dyer, *Nature* 398 (1999) 51.
- [14] J.H. Strickler, W.W. Webb, *SPIE Proc.* 1398 (1990) 107.
- [15] S. Maruo, S. Nakamura, S. Kawata, *Opt. Lett.* 22 (1997) 132.
- [16] A.S. Dvornikov, P.M. Rentzepis, *Opt. Commun.* 119 (1995) 341.
- [17] D.A. Parthenopoulos, P.M. Rentzepis, *Science* 245 (1989) 843.
- [18] H.B. Sun, S. Matsuo, H. Misawa, *Appl. Phys. Lett.* 74 (1999) 786.
- [19] Z.Q. Liu, Q. Fang, D.X. Cao, D. Wang, G.B. Xu, *Org. Lett.* 17 (2004) 2933.
- [20] P. Norman, Y. Luo, H. Ågren, *J. Chem. Phys.* 111 (1999) 7758.
- [21] C.K. Wang, P. Macak, Y. Luo, H. Ågren, *J. Chem. Phys.* 114 (2001) 9813.
- [22] K. Zhao, *J. Chem. Phys.* 126 (2007) 204509.
- [23] M. Albota, D. Beljonne, J.-L. Bredas, J.E. Ehrlich, W.W. Webb, X.-L. Wu, C. Xu, *Science* 281 (1998) 1653.
- [24] B.A. Reinhardt, L.L. Brott, S.J. Clarson, A.G. Dillard, J.C. Bhatt, R. Kannan, L. Yuan, G.S. He, P.N. Prasad, *Chem. Mater.* 10 (1998) 1863.
- [25] L. Li, N. Yuan, P. Wang, Y. Wu, Y. Song, Z. Chen, C. He, *J. Phys. Org. Chem.* 25 (2012) 872.
- [26] H. Fu, H. Wu, X. Hou, F. Xiao, *Syn. Metals* 156 (2006) 809.
- [27] W. Zhu, X. Meng, Y. Yang, Q. Zhang, Y. Xie, *Chem.: Eur. J.* 16 (2010) 899.
- [28] I. Ftilis, M. Fakis, I. Polyzos, V. Giannetas, P. Persephonis, *Chem. Phys. Lett.* 447 (2007) 300.
- [29] G. Brizius, S. Kroth, U.H.F. Bunz, *Macromolecules* 35 (2002) 5317.
- [30] D. Velasco, S. Castellanos, M. López, F.L. Calahorra, E. Brillas, L. Julia, *J. Org. Chem.* 72 (2007) 7523.
- [31] J. Ding, J. Gao, Y. Cheng, Z. Xie, *Adv. Funct. Mater.* 16 (2006) 575.
- [32] Y. Yamaguchi, S. Kobayashi, T. Wakamiya, Y. Matsubara, Z. Yoshida, *Angew. Chem. Int. Ed.* 44 (2005) 7040.
- [33] S. Tirapattur, M. Belletête, M. Leclerc, G. Durocher, *J. Mol. Struct.* 625 (2003) 141.
- [34] M. Belletête, M. Bédard, M. Leclerc, G. Durocher, *J. Mol. Struct.* 679 (2004) 9.
- [35] M. Belletête, J.F. Morin, M. Leclerc, G. Durocher, *J. Phys. Chem. A* 109 (2005) 6953.
- [36] L. Li, Y.Q. Wu, Q.L. Zhou, C.Y. He, *J. Phys. Org. Chem.* 25 (2012) 362.
- [37] G.S. He, J.D. Bhawalkar, P.N. Prasad, *Opt. Lett.* 20 (1995) 1524.
- [38] C. Wang, L. Liu, W.B. Ma, Z.H. Zhou, *Optik* 116 (2005) 75.
- [39] A.D. Becke, *J. Chem. Phys.* 98 (1993) 5648.
- [40] C. Lee, W. Yang, R.G. Parr, *Phys. Rev. B* 37 (1988) 785.
- [41] R. Ditchfield, W.J. Hehre, J.A. Pople, *J. Chem. Phys.* 54 (1971) 724.
- [42] X. Zhou, J.K. Feng, A.M. Ren, *Chem. Phys. Lett.* 403 (2005) 7.